FAST FOREST MONITORING ALGORITHM FOR LANDSAT TM/ETM+ IMAGE DATA

Nguyen Dinh DUONG[a], Nguyen Mai PHUONG[b]

[a] Institute of Geography
18 Hoang Quoc Viet Rd., Cau Giay, Hanoi, Vietnam;
Tel: +84 -04-37562417; Fax. +66 -04-38361192
E-mail: duong.nguyen2007@gmail.com

[b] ICRAF Vietnam office
8 Lot 13A, Trung Hoa, Yen Hoa, Cau Giay, Hanoi, Vietnam
Email: n.maiphuong@cgiar.org

KEY WORDS: Landsat TM/ETM+, Algorithm, Forest extraction, Spectral pattern analysis

Abstract: Forests are vital earth ecosystems that provide a variety of ecological, social and economic values. Deforestation and forest degradation, however, have made forests vulnerable, causing significant impacts on global climate. Forest resources in Vietnam are decreasing dramatically, especially in Kon Tum province which is located in Central Highlands of Vietnam. Quantifying spatial forest change information is important for assessing influences of human activities and environmental changes on ecosystem sustainability. This is a report on development of new forest monitoring algorithm using Landsat TM and ETM+ dataset. The algorithm allows fast forest classification and change detection. The algorithm was developed based on usage shape of spectral reflectance curve. Spectral reflectance curve of similar ground objects is encoded using modulation of the curve and using the modulation of spectral reflectance curve forest can be fast and almost automatically extracted from the Landsat TM and ETM+ image. An area of Kon Tum province of Vietnam has been used as test site. Validation was made by field work conducted in 2012 and comparison with latest land use map.

1. INTRODUCTION

Forest is very important for the earth environment. Recently scientists over the world have agreed that forest has strong effects on greenhouse gases (Fearnside, 2000), biodiversity (Lawton et al., 1998;Pimm & Raven, 2000), and regional climate (Salati & Nobre, 1991). Forest management requires timely and reliable information on forest status and its temporal dynamics. Satellite image has been used for forest monitoring and inventory for decades (Hansen et al., 2010a, 2010b, 2008). Especially multichannel satellite image data with spectral information about vegetation in near infrared and short wave infrared regions has been recognized to be an effective tool for detecting forest extents and changes in countrywide, regional and global scales (Langner et al., 2007; Tottrup et al., 2007; Xiao et al., 2009). Forest monitoring can be carried out by low spatial and high temporal resolution satellite images such as NOAA, SPOT Vegetation and MODIS (Achard & Estreguil, 1995; Stibig &Malingreau, 2003; Stibig et al., 2004; Langner et al., 2007; Tottrup et al., 2007; Xiao et al., 2009) or by high spatial and low temporal resolution satellite image like Landsat TM/ETM+ (Coppin & Bauer, 1994; Hall, Botkin, Strebel, &Goetz, 1991; Jha & Unni, 1994; Vogelmann & Rock, 1988). Advantages of Landsat data is that the historical archive of imagery dating back to the launch of ERTS in 1972 provides a unique and invaluable data source for tracking forest cover dynamics. But due to small coverage there are also many disadvantages rooting from local calibration issues and vegetation phenology (Woodcok et al., 2000).

The purpose of this paper is to develop a fast algorithm for forest extraction using spectral patterns which could be considered as invariant and stable in both time and location domain. The algorithm should work with both terrain corrected and surface reflectance product of the Landsat TM/ETM+. The authors also aim to application for the data of the future LCDM. This is a preliminary development of algorithm which can automatically separate forest from cropland and other non forest cover. The algorithm had been tested with Landsat TM/ETM+ surface reflectance and terrain corrected products from 2001, 2004 and 2010 in Kon Tum province in Vietnam.

2. MATERIAL AND METHOD

The Landsat TM and ETM+ image data has seven spectral channels as listed in table 1. For this research only six channels in visible spectrum will be used and they are numbered in sequence from 1 to 6. The thermal channel will not be used.

Each pixel in the image is described by a vector of 6 components b_i where i=1, 6 and b_i is digital number DN in each spectral channels. The value DN is converted to top of atmosphere reflectance L_λ based on the calibration coefficients, sun elevation, Earth-sun distance and the mean exoatmospheric solar radiance for each spectral channel (Chander 2009).

$$\rho_\lambda = \frac{\pi L_\lambda d^2}{ESUN_\lambda \cos\theta_s}$$

Where

ρ_λ=Planetary TOA reflectance [unit less]
π = Mathematical constant
L_λ = Spectral radiance at the sensor's aperture [W/(m^{2}srμm)]
d= Earth-Sun distance [astronomical units]
$ESUN_\lambda$= Mean exoatmospheric solar irradiance [W/(m^{2}μm)]
θ_s= Solar zenith angle [degrees]

Table 1: Spectral characteristics of Landsat TM/ETM+ image data in visible channels

Band number	TM sensor	ETM+ sensor
1	0.45-0.52	0.45-0.515
2	0.52-0.60	0.525-0.605
3	0.63-0.69	0.63-0.69
4	0.76-0.90	0.75-0.90
5	1.55-1.75	1.55-1.75
6	2.08-2.35	2.09-2.35

The authors proposed a fast forest extraction algorithm for such normalized data set. The algorithm is based on analysis of spectral pattern of the spectral reflectance curve. Spectral patterns of relevant ground objects could be constructed using the USGS 06 spectral library. The USGS spectral library has been developed by continuous spectral measuring from UV to mid infrared wave length (Clark et al. 2007). In order to simulate Landsat TM/ETM+ spectral reflectance the spectrum in the USGS 06 library has been resampled to 6 visible channels by averaging spectral values in respective channel width. Figure 1 show spectral reflectance curves of lawn grass, open sea water, dry grass and brick constructed by resampling approach.

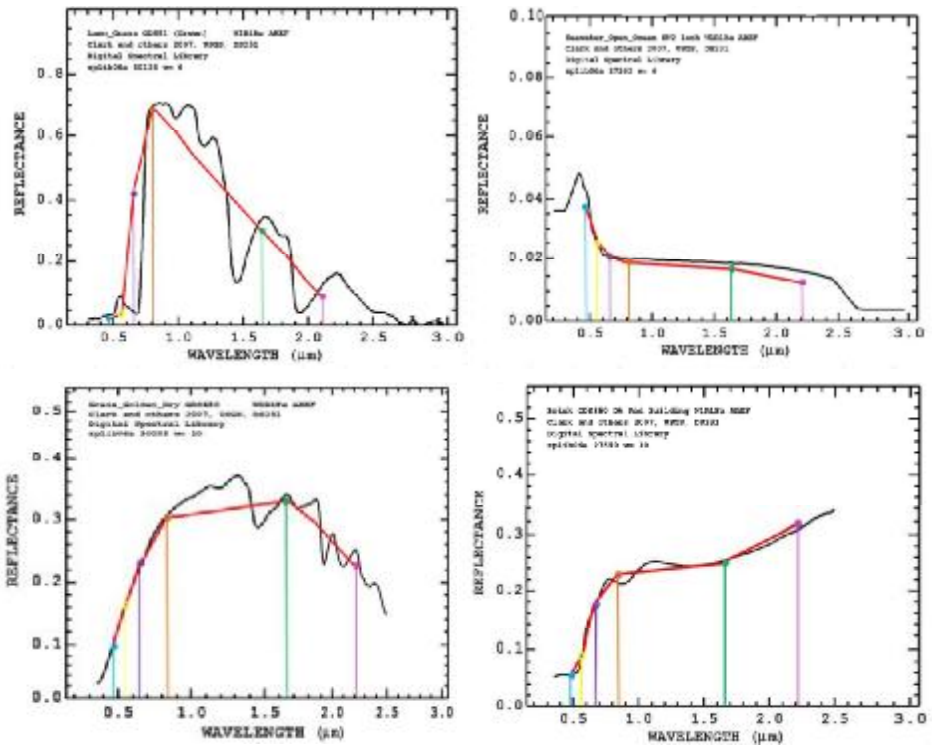

Figure 1: Construction of spectral reflectance curves by resampling of spectral values in USGS 06 spectral library

It is obvious that different ground objects have different patterns of the spectral reflectance curves and the spectral patterns could be used for object extraction and classification (Duong 1997).

In order to use the spectral pattern for spectral classification the first step to be done is encoding of the spectral pattern. One of encoding methods is to compare relative positions of vertices of the reflectance curve (Duong 1997). Let C_{ij} is a value indicating relative positions of vertices ρ_i and ρ_j on the spectral reflectance curve, C_{ij} is 0 when $\rho_i < \rho_j$, 1 when $\rho_i = \rho_j$ and 2 if $\rho_i > \rho_j$. For a data set with n spectral channels we need a string of $(n\text{-}1)n/2$ digits to encode the shape of the spectral reflectance curve. Maximal number of spectral patterns of the data set is $3^{(n-1)n/2}$ (Duong 1997). In case of Landsat TM/ETM+ image data if 6 spectral channels will be used for description of a ground object we need string of 15 digits for encoding the spectral reflectance curve. Number of spectral pattern types could reach 14,348,907. For forest extraction purpose only 4 spectral channels ρ_2, ρ_3, ρ_4 and ρ_5 without blue channel will be used. Therefore code of spectral pattern is consisted of 6 digits only and number of spectral patterns reduces to 729.

Using the USGS spectral library we can find out that spectral reflectance curve of vegetation after encoding is described by a number 200002. Because forest is only one component of vegetation cover and so the pixel which has spectral pattern 200002 could be forest or shrub or other vegetation types. But the main difference between forest and other vegetation could be seen in canopy structure. Forest usually has complicated canopy structure which is not homogeneous and tending to be affected by shadows. The Total reflected radiance index – TRRI (Duong 1998) of forest is always smaller than of other ground objects (Duong 1997). By applying thresholds for TRRI there is possibility of separation of forest from other vegetation. However, still some bush and other vegetation cover due to low background reflectance have the same TRRI like matured forest so the authors introduce Tree Canopy Index – TCI which can separate quite good forest from other vegetation cover. The TCI is computed by the following formula

$$TCI = (\rho_4 - \rho_5)/(\rho_5 - \rho_6)$$

In general the greater is the TCI the more complex canopy the vegetation community will have. In case ρ_4 is nearly equal ρ_5 then TCI is small and when ρ_5 is nearly equal ρ_6 then TCI is very big. Fortunately difference between ρ_5 and ρ_6 for forest is always remarkable. To avoid these extreme cases during computation ratio ρ_4/ρ_5 is used to filter out other objects from forest.

Figure 2 shows example of scatter plots for pixels of spectral pattern 200002 of a Landsat TM image. The vertical axis is for TRRI values and the horizontal axis shows TCI values. Figure 2a displays spectral plot for all pixels without differences in spectral patterns. Figure 2b shows spectral plot for pixels of pattern 200002 only after filtering pixels which do not satisfy the tree canopy index thresholds. Color composite used in these figures is R, G, B =6, 4, 3. Figure 2a shows all ground objects including water, vegetation and bare land. By using the vegetation spectral pattern it is easy to separate vegetation from the other objects. The relation between TRRI and TCI is complex. One TRRI value can relate to many TCI values and vice versa one TCI value relates to many TRRI values. However, for purpose of separation of forest from other land cover categories it is possible to rely only on TRRI and TCI.

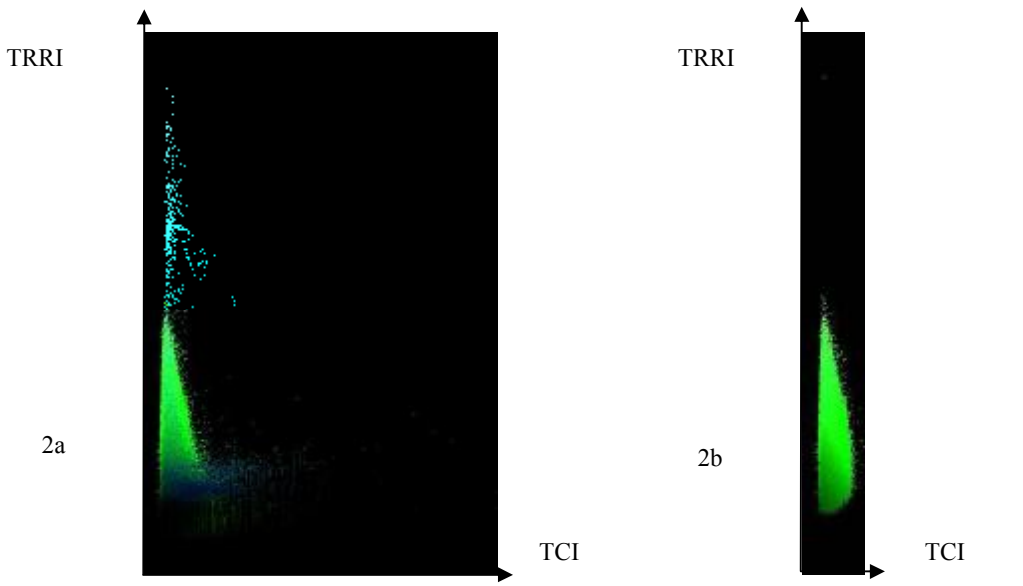

Figure 2: Scatter plots of all pixels in Landsat TM image (left) and for pixels with spectral pattern 200002 (right)

Algorithm for fast forest extraction from Landsat TM/ETM+ has been developed based on vegetation spectral pattern 20002, total reflected radian index TRRI and tree canopy index TCI. Block diagram of the algorithm is shown in figure 3.

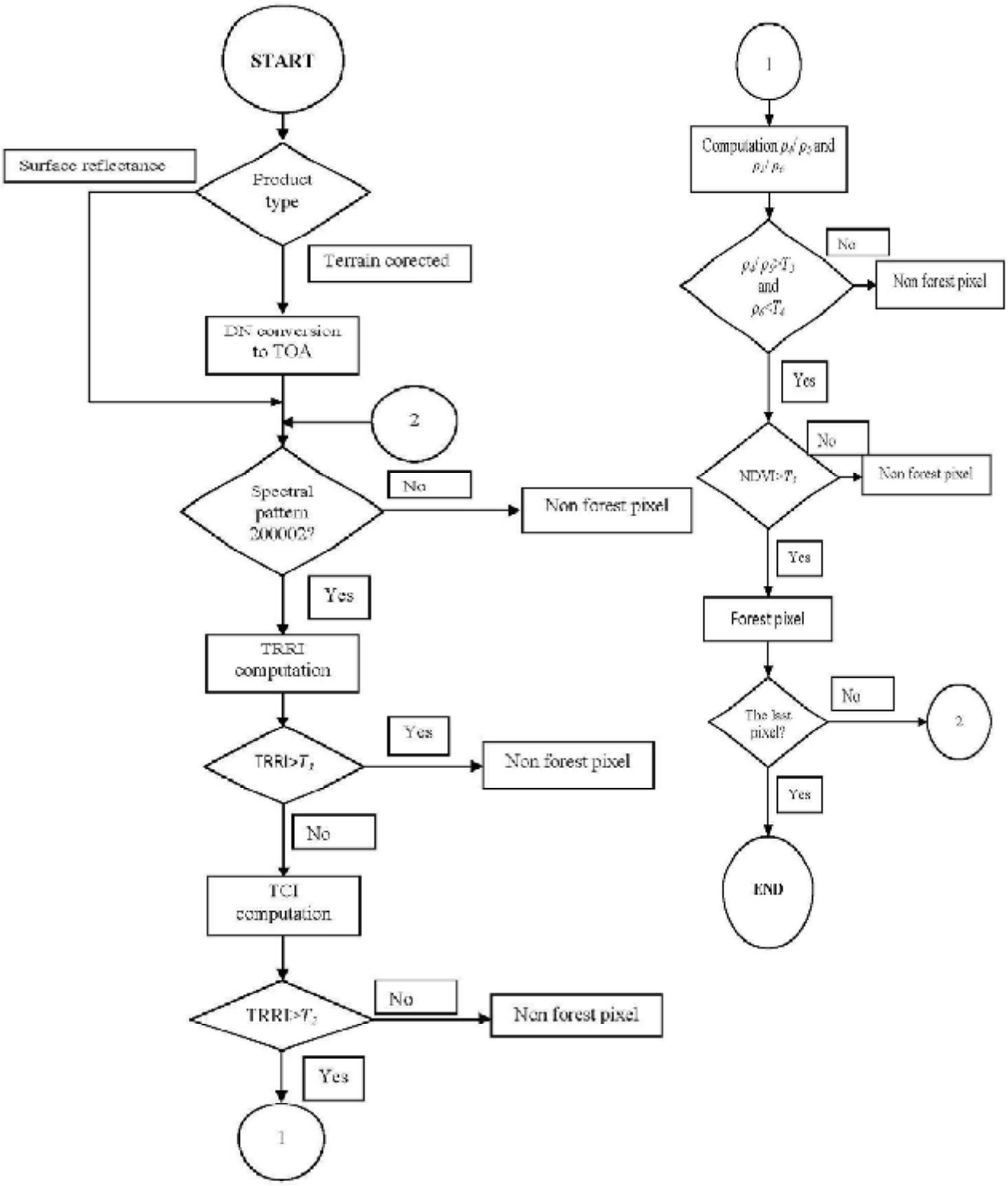

Figure 3: Fast forest extraction algorithm for Landsat TM/ETM+

In fact this algorithm is based on five thresholds T_1, T_2, T_3, T_4 and T_5 for TRRI and TCI. T_1 is threshold for TRRI to separate cloud from forest. T_2 is threshold for TCI to divide ground objects to forest and non forest areas. T_3 is threshold for ratio $\rho_4/\ \rho_5$, T_4 is reflectance for channels 6 and T_5 is threshold of NDVI. All pixels which do not

satisfy these thresholds will be classified as non forest. By experiments the authors suggested values for thresholds T_1, T_2, T_3, T_4 and T_5 as shown in table 2.

Table 2: Threshold values for T_1, T_2, T_3, T_4 and T_5

Parameters	Thresholds for L1T product	Thresholds for surface reflectance product
T_1	1.59	2.0
T_2	1.8	1.2
T_3	1.8	1.6
T_4	0.065	0.065
T_5	0.65	0.80

Data used for this study are standard Landsat TM/ETM+ products observed in 2001, 2004 and 2010 over Kon Tum province, Vietnam. Details of technical parameters of data are given in the table 3.

Table 3: List of data used

Granule ID	Date of observation	Date of processing	Product name
p124r050_7dx20011017.SR.ESDR	17/10/2001	26/03/2011	Landsat Surface Reflectance
p124r050_7dx20040228.SR.ESDR	28/02/2004	29/03/2011	Landsat Surface Reflectance
L72124050_05020100316	16/03/2010	6/02/2012	Terrain corrected

All these products have been terrain corrected. Data from 2001 and 2004 are surface reflectance product. These data are copyrighted to NASA Landsat program, USGS Sioux Falls. Conversion of DN to TOA was necessary for only data from 16/3/2010. Coefficients used for conversion of DN to TOA are given in table 4.

Table 4: Calibration coefficients and parameters for conversion of DN to TOA for Landsat ETM+ of 16/3/2010

Band	Gain	Bias	Exoatmospheric coefficient
1	0.778740	-6.98	1997
2	0.798819	-7.20	1812
3	0.621654	-5.62	1533
4	0.969291	-6.07	1039
5	0.126220	-1.13	230.8
6	0.043898	-0.39	84.90
Earth-sun distance	0.99474	Sun elevation	56.9712706

Figure 4 shows color composites 6,4, 3 for used data. The data from 2004 and 2010 were taken during dry season so it is quite easy to detect forest and non forest areas while in data from 2001 taken in late rainy season, both vegetation covers: forest and agricultural cultivation are dense and it is very difficult visually to separate each from other.

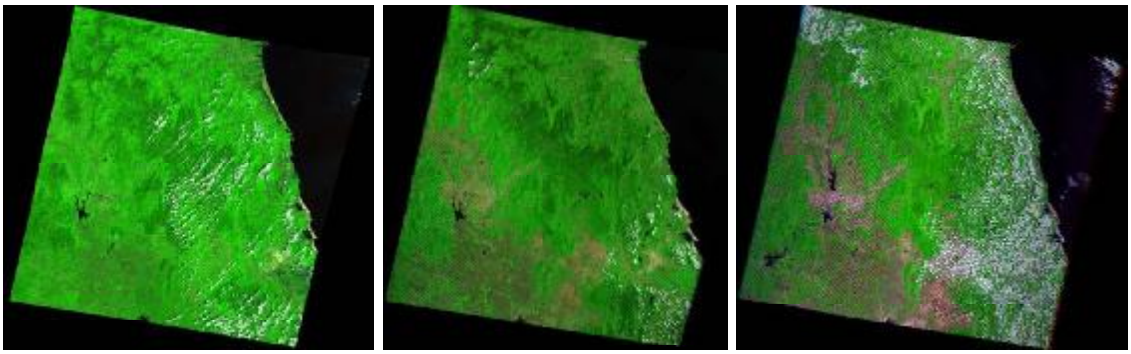

Figure 4: Color composites of used data 2001 (left), 2004 (middle) and 2010 (right)

3. RESULT AND DISCUSSION

After applying the above algorithm with thresholds given in the table 4 forest covers from the three Landsat scenes have been extracted. Let us start with small image subset from 2001 (see figure 5a). By visual interpretation it is very easily to recognize forest on mountains while on low land the agricultural cultivation like rice crop dominates. There are also industrial tree plantation such as coffee and rubber in different growth stages. Forest in this subset allocates mainly in the left with dark green color, agricultural cultivation distributes on right site with different light green shades. Figure 5b shows analysis result using spectral pattern 200002 and the TCI. As we can see that still many plantation cover remain so we need to remove them by using the thresholds of NDVI and channel 6 and we can achieve result as in figure 5c. Based on experiments we found out that reflectance of forest cover is usually smaller than reflectance of bush cover in channel 6. However some bush or shrub covers have also low reflectance in channel 6 so we need to use NDVI to separate shrub and bush from forest. Figure 6d shows final result of forest extraction overlaid on color composite 4, 3, 2. By visual interpretation we can see that non forest cover has been almost completely removed and in the image remains only forest cover.

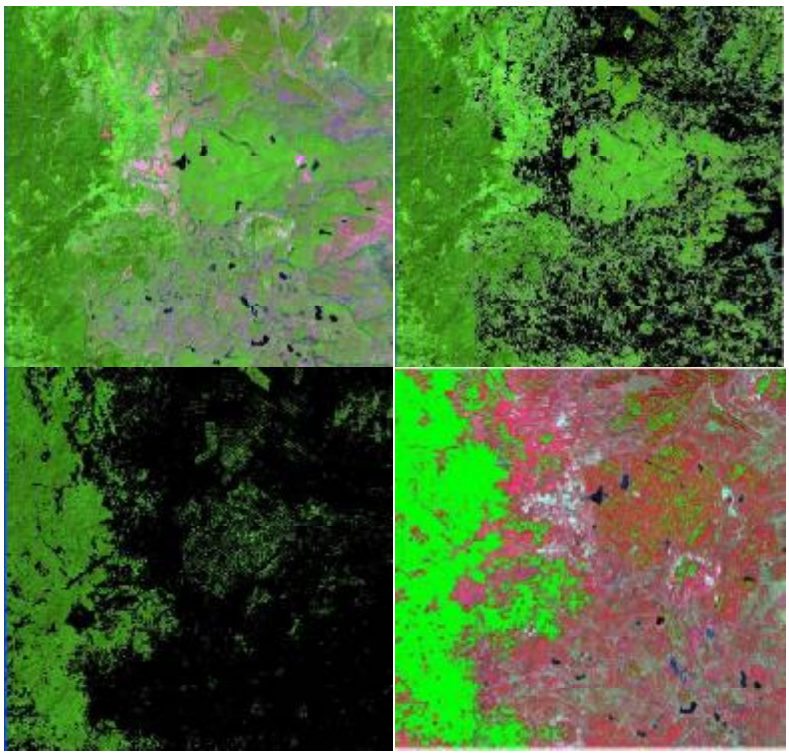

Figure 5: Forest extraction using the proposed algorithm for a subset of Landsat TM from 2001

Figure 6: Differences in canopy structure for natural forest (left) and forest plantation (right)

Differences between natural and planted forest can be seen in figure 6. Left image shows natural forest and right image shows rubber plantation.

By visual interpretation we can recognize reduction of forest cover and expanding of agricultural cultivation. This trend is clearer by using small image subset as shown in figure 8. In 2001 forest distributes on both low land and up land but in 2004 it has been shrink to mountain area and in 2010 forest remain only on upper parts of mountains. The deforestation is obvious through field GPS photos which have been taken in March 2012 (figure 9).
Figure 7 shows forest extraction for all three Landsat scenes from 2001, 2004 and 2010 and enlargement in figure 8 shows more details in forest cover change.

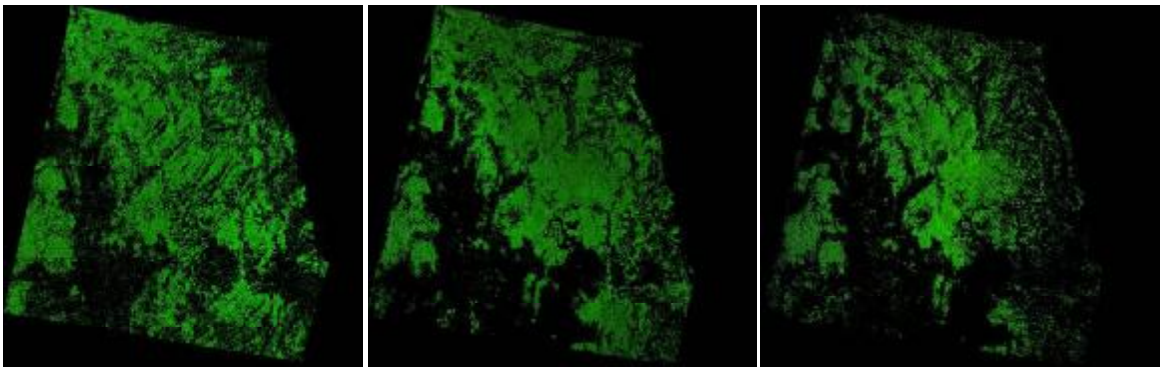

Figure 7: Forest covers from 2001 (left), 2004 (midle) and 2010 (right) for whole Landsat scenses

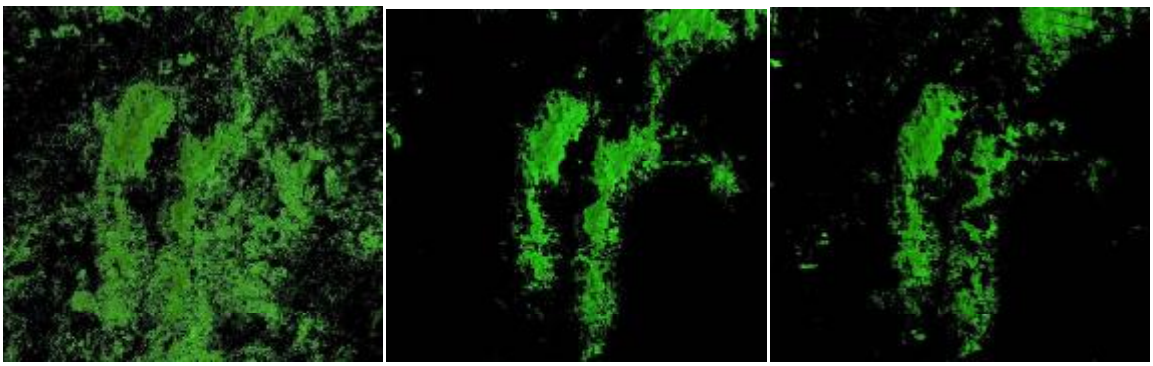

Figure 8: Subset of study area showing details in forest cover changes from 2001 (left) to 2004 (middle) and 2010 (right)

Figure 9: Deforestation for agricultural cultivation development as observed on ground

Figure 10 shows linkage between classified Landsat 2010 image and GPS photos taken in March 2012. Line gaps in the Landsat image were not removed because gap removing could lead to distortion of spectral characteristics of image data which can result in miss classification. By fast comparison checking between classification result and field photos the authors could confirm that the proposed algorithm works quite well.

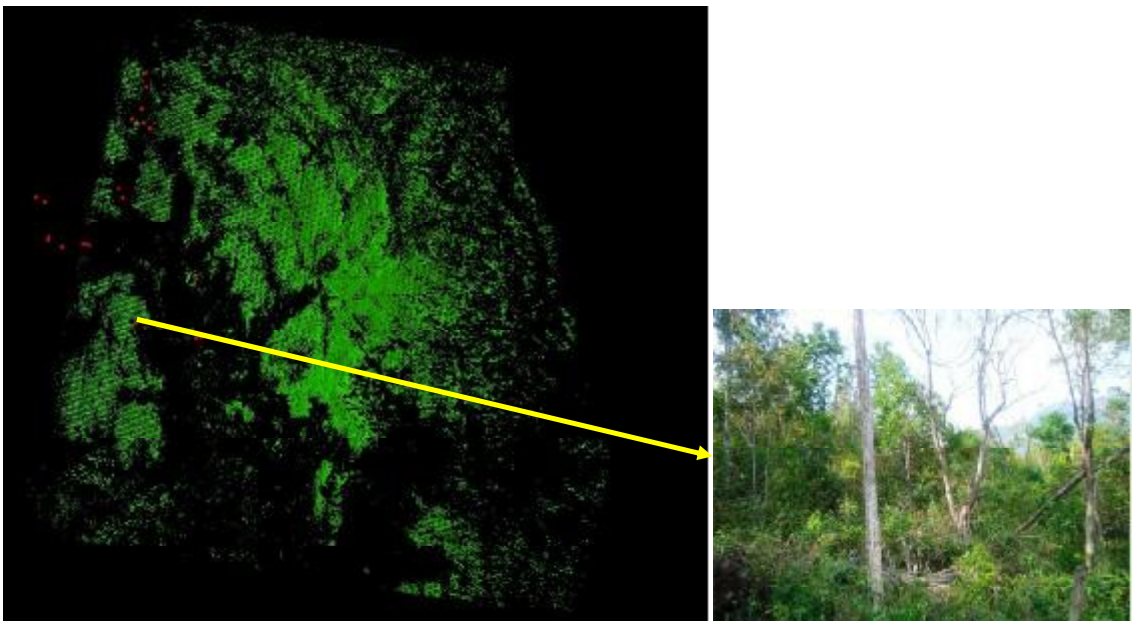

Figure 10: Forest cover from 2010 and field GPS photos marked as red dots for quick validation

4. CONCLUSION

Automated fast forest extraction from single date multispectral image in general and from Landsat image data in particular is important issue. Due to vegetation phenology and seasonal change of cropland automated forest detection is still challenge. The problem is resolved by using time series image data of low spatial resolution like MODIS but it remains still for medium spatial multispectral data like Landsat where it is not available high temporal series data. The algorithm proposed in this paper is one of attempts for fast extraction of forest cover using single date and high spatial resolution image data without auxiliary information. The algorithm works with both Landsat TM/ETM+ terrain corrected and surface reflectance products. It is expected that it will work with the future Landsat 8 products as well. The algorithm was developed using spectral pattern of four channels: green, red, infrared and short wave infrared. In addition to the spectral pattern indices like TRRI and TCI have been used to separate forest from bush and cropland. Study had been carried out in Kon Tum province. Algorithm development had been supported by field work in March 2012. The fast forest extraction algorithm could be used for analysis of the GLS surface reflectance product of USGS. The GLS SR is quite stable and it is good dataset for base line forest mapping in large area

REFERENCES:

Chander, G., Markham, B.L., and Helder, D.L., (2009). Summary of current radiometric calibration coefficients for Landsat MSS, TM, ETM+, and EO-1 ALI sensors, Remote Sensing of Environment, v. 113, no. 5, p. 893-903.

Clark, R.N., Swayze, G.A., Wise, R., Livo, E., Hoefen, T., Kokaly, R., Sutley, S.J., (2007). USGS digital spectral library splib06a: U.S. Geological Survey, Digital Data Series 231

Coppin, P. R., & Bauer, M. E. (1994). Processing of multitemporal Landsat TM imagery to optimize extraction of forest cover change features. IEEE Transactions on Geoscience and Remote Sensing, 32 (4), 918– 927.

Duong N. D., (1997). Graphical Analysis Of Spectral Reflectance Curve. Proceedings Of The 18th Asian Conference On Remote Sensing, 20-24 October 1997. Kuala Lumpur, Malaysia.

Duong N. D., (1997). Semi-Automatic Land Cover Classification Using ADEOS/AVNIR Multispectral Data. Proceedings Of The 18th Asian Conference On Remote Sensing, 20-24 October, 1997. Kuala Lumpur, Malaysia.

Duong N. D., (1998). Total Reflectance Radiance Index – An Index To Support Land Cover Classification. Proceedings Of The 19th Asian Conference On Remote Sensing, 16-20 November, 1998. Manila, Philippine.

Duong N. D., (1999). Monitoring of Forest Cover Change in Tanh Linh District, Binh Thuan Province, Vietnam by Multi-Temporal Landsat TM Data. Proceedings Of The 20th Asian Conference On Remote Sensing, 22-26 November, 1999. Hong Kong, China.

Duong N. D., (2000). Land Cover Category Definition by Image Invariants for Automated Classification. International Archives of Photogrammetry and Remote Sensing. Vol. XXXIII, Part B7/3, Commission VII. ISPRS 2000 Amsterdam, the Netherlands.

Fearnside, P. M. (2000). Global warming and tropical land-use change: Greenhouse gas emissions from biomass burning, decomposition and soils in forest conversion, shifting cultivation and secondary vegetation. Climatic Change, 46, 115–158.

Hall, F. G., Botkin, D. B., Strebel, D. E., & Goetz, S. J. (1991). Large-scale patterns of forest succession as determined by remote sensing. Ecology, 72, 628– 640.

Hansen, M. C., Stehman, S. V., & Potapov, P. V. (2010a). Quantification of global gross forest cover loss. Proceedings of the National Academy of Sciences of the United States of America, 107, 8650–8655.

Hansen, M. C., Stehman, S. V., & Potapov, P. V. (2010b). Reply to Wernick et al.: Global scale quantification of forest change. Proceedings of the National Academy of Sciences of the United States of America, 107, E148-E148.

Hansen, M. C., Stehman, S. V., Potapov, P. V., Loveland, T. R., Townshend, J. R. G., DeFries, R. S., et al. (2008). Humid tropical forest clearing from 2000 to 2005 quantified by using multitemporal and multiresolution remotely sensed data. Proceedings of the National Academy of Sciences of the United States of America, 105, 9439–9444.

Jha, C. S., & Unni, N. V. M. (1994). Digital change detection of forest conversion of a dry tropical Indian forest region. International Journal of Remote Sensing, 15 (13), 2543– 2552.

Langner, A., Miettinen, J., & Siegert, F. (2007). Land cover change 2002–2005 in Borneo and the role of fire derived from MODIS imagery. Global Change Biology, 13, 2329–2340.

Lawton, J. H., Bignell, D. E., Bolton, B., Bloemers, G. F., Eggleton, P., Hammond, P. M., et al. (1998). Biodiversity inventories, indicator taxa and effects of habitat modification in tropical forest. Nature, 391, 72–76.

Pimm, S. L., & Raven, P. (2000). Biodiversity — Extinction by numbers. Nature, 403, 843–845.

Salati, E., & Nobre, C. A. (1991). Possible climatic impacts of tropical deforestation. Climatic Change, 19, 177–196.

Tottrup, C., Rasmussen, M. S., Eklundh, L., & Jonsson, P. (2007). Mapping fractional forest cover across the highlands of mainland Southeast Asia using MODIS data and regression tree modelling. International Journal of Remote Sensing, 28, 23–46.

Vogelmann, J. E., & Rock, B. N. (1988). Assessing forest damage in high elevation coniferous forests in Vermont and New Hampshire using Thematic Mapper data. Remote Sensing of Environment, 24, 227– 246.

Curtis E. Woodcock, Scott A. Macomber, Mary Pax-Lenney, Warren B. Cohen (2000). Monitoring large areas for forest change using Landsat: Generalization across space, time and Landsat sensors. Remote Sensing of Environment, 78, 194– 203.

Xiao, X., Biradar, C., Czarnecki, C., Alabi, T., & Keller, M. (2009). A simple algorithm for large-scale mapping of evergreen forests in tropical America, Africa and Asia. Remote Sensing, 1, 355–374.